

Los Alamos National Laboratory is operated by the University of California for the United States Department of Energy under contract W-7405-ENG-36

TITLE: MEXICO CITY OZONE CONCENTRATIONS AS A FUNCTION OF
READILY-AVAILABLE METEOROLOGICAL PARAMETERS

AUTHOR(S): Michael J. Brown

SUBMITTED TO: IMP, Mexico City, Mexico
February 1994
Mexico City Air Quality Research Initiative

DISCLAIMER

This report was prepared as an account of work sponsored by an agency of the United States Government. Neither the United States Government nor any agency thereof, nor any of their employees, makes any warranty, express or implied, or assumes any legal liability or responsibility for the accuracy, completeness, or usefulness of any information, apparatus, product, or process disclosed, or represents that its use would not infringe privately owned rights. Reference herein to any specific commercial product, process, or service by trade name, trademark, manufacturer, or otherwise does not necessarily constitute or imply its endorsement, recommendation, or favoring by the United States Government or any agency thereof. The views and opinions of authors expressed herein do not necessarily state or reflect those of the United States Government or any agency thereof.

By acceptance of this article, the publisher recognizes that the U.S. Government retains a nonexclusive, royalty-free license to publish or reproduce the published form of this contribution, or to allow others to do so, for U.S. Government purposes.

The Los Alamos National Laboratory requests that the publisher identify this article as work performed under the auspices of the U.S. Department of Energy

Los Alamos

MASTER
Los Alamos National Laboratory
Los Alamos, New Mexico 87545

Mexico City Ozone Concentrations As A Function Of Readily-Available Meteorological Parameters

Michael J. Brown

**Los Alamos National Laboratories
Group TSA-4, MS B299
Energy and Environmental Assessment
Los Alamos, NM, 87545**

Abstract. Daily maximum ozone concentrations measured at four sites within the Mexico City basin during the winter months are plotted as functions of different meteorological parameters that are routinely measured at surface stations. We found that ozone concentrations are most strongly correlated to the increase in daytime temperature and the maximum daytime wind speed. We also discovered that high ozone values at the sites in the southern end of the basin occur when winds come out of the northeast. In contrast, wind direction was found to be uncorrelated with high ozone values at the northern sites. From straightforward combinations of the meteorological variables, we derived some simple rules for estimating lower and upper bounds on the ozone concentration. Scatter in the data was too large to give significance to best-fit equations and statistics. Additionally, a small rawinsonde data set was used to investigate ozone's dependence on boundary-layer height and near-surface temperature gradient. Results were inconclusive, however, due to the small size of the data set.

1. Introduction

Mexico City has a serious ozone air pollution problem. In the five year period from 1988 to 1992, ozone levels within Mexico City exceeded the one-hour Mexican air quality standard of 110 parts per billion (ppb) an average of 335 days out of each year. In that same period, a one-hour average of 230 ppb was exceeded an average of 94 days per year. These high ozone levels stem, in part, from Mexico City's large population (approximately 20 million people) and from its location in a basin surrounded on three sides by mountains. In an effort to help deal with Mexico City's air pollution problem, the Instituto del Petroleo and Los Alamos National Laboratory have teamed together to model and measure the air flow, pollutant dispersion, and air chemistry in the Mexico City basin. A description of these efforts can be found in Williams et al. (1993).

This paper deals with one small aspect of the study: the correlation of daily maximum hourly-averaged ozone concentrations with routine meteorological measurements. Our analysis will be confined to the winter months when severe ozone episodes commonly occur. In section 2, we will briefly review the geography of the Mexico City basin, the locations of the monitoring stations, and the types of meteorological and concentration instrumentation. We list our assumptions and analysis methods in section 3. We will then present our results in two parts: the first will compare ozone and meteorological measurements made at four surface-level stations and the second will utilize upper-air meteorological measurements in the comparison at the same four surface-level stations. From the correlations, several simple relationships will be derived which may prove to be applicable to short-term forecasting of lower and upper bounds on the ozone concentration.

2. Description of geography, monitoring sites, and instrumentation

Mexico City lies at approximately 7500 feet above sea level in the southwestern portion of the Valley of Mexico. Twelve-thousand foot mountains form a U-shaped barrier on three sides, while an opening exists to the north. Individual peaks extend up to 17,000 feet. Meteorological parameters and air pollutant concentrations are measured at twenty-five monitoring sites operated by the

Secretariat of Social Development. For our analysis, we have chosen four sites that measure wind speed, wind direction, temperature, relative humidity, and ozone. These sites are denoted by the letters F, L, T, and X and are located in the northwest, northeast, southeast, and central sections of the city (see fig. 1). Four months of data were used for this study (Jan. 1991, Dec. 1991, Jan. 1992, and Feb. 1992).

The monitoring sites were equipped with cup anemometers, wind vanes, and temperature and dewpoint sensors. Ozone was measured using chemiluminescent analyzers. Wind detection instruments were mounted on small towers at a height of ten meters above the surface or rooftop. Measurements were sampled at one minute intervals and hourly averages were recorded on data loggers (note: wind speed and direction were obtained by scalar averaging rather than by vector averaging; for typical turbulence intensities, however, experimental measurements showed that the one-hour scalar averaging resulted in only a five to thirty percent smaller wind speed than vector averaging).

Additionally, rawinsonde measurements were made at the Mexico City airport which is denoted by the letter Y. Wind speed, wind direction, temperature, pressure and moisture were measured at approximately seventy-five meter intervals from the surface to a height of about five or ten kilometers. The averaging time for these measurements was a relatively short 15 to 30 seconds. Although these measurements were taken several times daily, only three weeks of data were made available to us (Feb. 8 - 28, 1991).

3. Assumptions and analysis methods

Ozone formation in the boundary layer is a complex photolytic chemical process which depends, in part, on the magnitude of solar radiation and the relative amounts of nitrogen oxides, nitrogen dioxides, and hydrocarbons (see, for example, Seinfeld, 1986). Without direct measurements of the weekly variation in the emissions of these chemical species, we made the simplifying assumption that the emissions were the same for each weekday. We threw out weekend data because of the possibility of different weekend traffic volume. Our analysis showed that correlations of ozone with various meteorological parameters improved when weekend data was not included.

Because direct measurements of solar insolation were not taken, we have attempted to account for ozone's dependence on sunlight by assuming that the amount of sunlight is proportional to the daytime temperature rise ΔT , which we define as the difference between the maximum and minimum daily temperatures (the former usually occurring between noon and 4 p.m. and the latter between 5 a.m. and 7 a.m.). However, ΔT may also be proportional to the convective strength of the boundary layer. Hence, a large ΔT may lead to an increase in ozone due to more solar radiation and at the same time may reduce ozone levels because of increased vertical mixing by the convective thermal cells. Note: in order for ΔT to be proportional to the amount of solar radiation, we must assume that the magnitude of energy transport and conversion processes, such as evaporation, advection, and heat flux into the ground, does not vary appreciably at each particular site during the study period.

A complete record of rainfall, which acts to wash out air pollution in the boundary layer, was not available to us. Rain events may be correlated with high values of relative humidity and smaller values of daytime temperature rise, which are both measurements that we do have. Fortunately, however, the winter months from December to February average a very low five to ten millimeters of rainfall per month. During February 1991, light rain events of one millimeter or less occurred three times, all during night hours.

From the four meteorological variables measured at the monitoring sites, we derived about ten quantities that may be relevant to the concentration levels of ozone. As mentioned above, we can calculate the daytime temperature rise ΔT , which we assume is proportional to the amount of sunshine available to drive the photochemical reaction. We computed a vector-averaged wind speed (i.e., the individual N-S and E-W wind components are averaged and then used to compute the wind speed) in order to determine the net movement of the ozone cloud within the Mexico City basin. Vector-averaged wind speeds were calculated for an eleven-hour "daytime" period between 7 a.m. and 6 p.m. and for an eighteen-hour "night and daytime" period between midnight and 6 p.m. (WS_{11v} and WS_{18v} , respectively). The eighteen-hour vector-average wind speed was computed in order to investigate the importance of night time transport of the ozone precursors. Vector-averaged wind directions were calculated because the prevailing wind direction may determine: 1) whether "fresh" or "contaminated" air is advected to a particular station or 2) whether the ozone cloud is flushed out of the basin opening to the north or trapped by the mountains to the west, south, and east. Additionally, we looked at the ratio of the vector- to scalar-averaged wind speed (where the scalar-average WS_s is determined by a summation of the wind speeds and then division by the total number of samples) as another possible measure of the net movement of the ozone cloud. A one-hour average maximum wind speed WS_{max} was determined from data taken between 7 a.m. and 6 p.m. The magnitude of the wind speed may be inversely proportional to ozone concentration for two reasons. First, from similarity theory the log-law velocity profile shows that for a given surface roughness the wind speed within the surface layer is proportional to the friction velocity (see, for example, Arya, 1988). The friction velocity is a measure of the intensity of turbulence or mixing potential of the surface layer and, therefore, is inversely proportional to surface-level concentration. Second, for a finite-sized area source, the Gaussian concentration equation indicates that the concentration is inversely proportional to wind speed (see, for example, Pasquill and Smith, 1983). In order to evaluate whether ozone concentrations at particular sites are affected by the prevailing wind direction, vector-average wind directions and the wind direction at the time of the wind speed maximum were determined. Lastly, eleven hour daytime averages were obtained for relative humidity and temperature.

For the three weeks of available upper-air rawinsonde data, we have computed the boundary-layer height and the vertical gradient of potential temperature near the surface. The boundary-layer height H_{bl} is indicative of the volume in which the ozone can be mixed and hence may be inversely proportional to ozone concentration. The daytime boundary-layer height is defined as the height at which $\Delta\theta/\Delta z$ first becomes larger than $0.006 \text{ } ^\circ\text{C}/m$, i.e., the height at which a moderate inversion first occurs. The vertical gradient of potential temperature $\Delta\theta/\Delta z$ near the

ground is proportional to the magnitude of the heat flux and hence may be indicative of the convective strength of the boundary layer. $\Delta\theta/\Delta z$ is based on the two lowest data points in the vertical profile, which are generally about 75 meters apart. We also computed vertically-integrated wind speeds, but found it had no better correlation with ozone concentration than surface-level wind speeds. Surface pressure and a near-surface bulk wind shear $\Delta u/\Delta z$ were also obtained from the rawinsonde data, however, we found no correlations with ozone concentration.

Finally, we point out that the various one-hour average meteorological measurements (e.g., maximum boundary-layer height, maximum wind speed) and the maximum ozone concentration may not have occurred at the same hour of the day. We have not used simultaneously-measured meteorological data in order that our results might be more applicable to simple forecasting, i.e., knowledge of when the maximum ozone concentration occurs introduces another level of complexity. It may be of some interest to note that the majority of maximum ozone concentrations take place between noon and four p.m., although, ozone maxima occasionally appear earlier in the day.

4. Results

a). Surface-level measurements at monitoring stations

In this section, we will compare the daily maximum one-hour average ozone concentrations at a particular monitoring station with the available surface-level meteorological measurements (wind speed, wind direction, relative humidity, and temperature) at that station. Initially, we will look at ozone as a function of just one variable using scatterplots and then later plot ozone versus combinations of the meteorological variables. For consolidation, we will sometimes plot results for only one station when results for other stations are similar or uneventful.

Figure 2 shows the daily maximum ozone plotted against different measures of wind speed for Station F. Clearly there is a lot of scatter in all four plots. Upon closer examination, however, some trends are apparent. For example, when the maximum daytime wind speed is less than about 5 m/s, ozone concentrations remain above 140 ppb (fig. 2a). When the vector-averaged wind speed is considered, there appears to be a mild tendency for lower wind speeds to be associated with higher ozone values and higher wind speeds to be associated with lower ozone values (figs. 2b and c). In the eighteen-hour vector-average case, we can see that ozone remains above 140 ppb for wind speeds below 1 m/s and remains below 100 ppb for wind speeds greater than 5 m/s (fig. 2c). The scalar-average wind speed gives poor correspondence with ozone levels (fig. 2d). Similar results are obtained for stations L, T, and X.

In fig. 3a, ozone is plotted as function of the daytime temperature increase ΔT for station F. Here, a relatively strong correlation is seen between high ozone levels and large ΔT and low ozone levels and small ΔT . This trend supports the idea that the daytime temperature increase is proportional to the amount of available sunlight, and that it is less strongly correlated with the boundary-layer convective strength. Figure 3b shows that ozone also correlates fairly well with the average daytime temperature. However, it seems that the correlation occurs because the average daytime temperature correlates fairly well with the daytime temperature increase (fig. 3c).

Figure 3d suggests that ozone levels remain small when the daytime-averaged relative humidity is above about fifty percent. This may be due to a higher likelihood of clouds (reducing the amount of sunlight) and/or rain (leading to the removal of ozone by washout) with higher relative humidity. For low relative humidity, the ozone levels vary widely.

The above results suggest plotting ozone concentration as a function of ΔT divided by the different measures of wind speed. Figure 4 shows ozone versus $\Delta T/WS_{11}$, $\Delta T/WS_{18v}$, $\Delta T/WS_{max}$, and $\Delta T/(WS_{18v}/WS_{18s})$ for station F. Clearly, the widest scatter is found when $\Delta T/(WS_{18v}/WS_{18s})$ is used as the independent variable (fig. 4c), suggesting that the vector- to scalar-average wind speed ratio is a poor indicator of ozone cloud transport. Grouping of data is fairly consistent with WS_{11v} , WS_{18v} , and WS_{max} as the denominators (figs. 4a, b, and c, respectively). However, if we look at all four stations, we see that using WS_{max} in the denominator yields better correlation than when using WS_{11v} or WS_{18v} (figs. 5, 6, and 7). Comparison of the scatterplots in figs. 6 and 7 show no significant improvement when the eighteen hour vector-averaged wind speed is used in place of the daytime (eleven hour) vector-averaged wind speed. This suggests that night time transport of ozone precursors may be insignificant. We can also see the impact of geographic location on the highest ozone levels, which are smallest at station L (located near the basin opening to the northeast) and largest at station T (located in the southwest corner of the basin and encompassed by nearby mountains to the south and west).

As mentioned in section 3, we believe that the eleven hour vector-average WS_{11v} contains information on the residence time of the ozone cloud over the monitoring station, while the one hour average WS_{max} gives an indication of the amount of dilution of the ozone cloud. Since both the short-term and long-term wind speed averages both affect the ozone concentration in different ways, we have experimented with numerous ways of combining their effects. We found that the best results were obtained with ozone plotted as a function of $\Delta T/(WS_{11v} + WS_{max})$. The scatterplots are shown in fig. 8 for all four stations. Clearly, the data shows a tighter grouping than in earlier figures. The most scatter is seen at station X (fig. 8d) located near the city center and may be a result of vacillating local changes in traffic emissions and building-influenced winds.

From fig. 8, some simple rules for ozone levels can be given which are generally applicable to all four stations:

$$\begin{aligned}
 & \text{if } \Delta T/(WS_{11v} + WS_{max}) < 0.5, & \text{then } O_3 < 100 \text{ ppb}; \\
 & \text{if } 0.5 < \Delta T/(WS_{11v} + WS_{max}) < 1.0, & \text{then } O_3 < 230 \text{ ppb}; \text{ and} \\
 & \text{if } \Delta T/(WS_{11v} + WS_{max}) > 1.0, & \text{then } O_3 > 100 \text{ ppb}.
 \end{aligned}$$

Notice that there are several data points that do not satisfy these rules. Unfortunately, a simple rule cannot be obtained from fig. 8 for the highest ozone concentrations. Since the daytime vector-average wind speed is a difficult variable to predict, a simple rule for ozone levels can also be obtained from fig. 5 using the more easily predicted ΔT and WS_{max} :

$$\text{if } \Delta T/WS_{max} > 1.5, \quad \text{then } O_3 > 100 \text{ ppb}.$$

We next look for relationships between ozone concentration and prevailing wind direction. In fig. 9, we have plotted the daily maximum ozone concentration as a function of the daytime vector-averaged wind direction. Results appear to be site specific. At station F, the data is widely scattered and no obvious grouping of data is seen (fig. 9a). We were expecting that surface-level winds from the north-northeast would bring fresh air and push the ozone cloud south, thus reducing ozone concentrations at the northwestern site. However, it turns out that relatively small wind speeds are present when the wind directions are between 0 and 120 degrees (fig. 10a), and hence, concentrations may be larger due to their inverse relationship with wind speed magnitude. At station L, the data is again widely scattered and we find two unexpected results (fig. 9b). First, when winds are between 30 and 150 degrees, i.e., they are coming from a relatively lighter populated region, the concentrations are all above 100 ppb. In this case, winds are somewhat lighter again (fig. 10b). Second, we find that all ozone values above 150 ppb occur when winds are between 30 and 180 degrees. Several possible explanations for the above results can be proposed, but not substantiated: 1) local emissions from vehicles may be transported by the wind from the north - a map of the Mexico City basin shows several major roadways to the north, northwest, and northeast of stations F and L; 2) the upper-level wind direction may be opposite to the surface-level winds, resulting in transport of polluted air aloft which is eventually mixed down to the surface in the afternoon by the growing mixed layer; 3) if blocked by the U-shaped mountains at the southern end of the basin, the north-northeasterly winds may recirculate the air from the city center back to the northern monitoring stations along the base of the mountains; 4) if the ozone cloud already fills the entire basin, north-northeasterly winds would result in negligible net movement of the ozone cloud due to the U-shaped mountains at the southern end; 5) winds originating from the north-northeast are slowed down by mountain blockage and the smaller winds lead to less dispersion of the locally-produced emissions; and/or 6) relatively fresh air is advected to the northern monitoring stations with somewhat lower ozone concentrations, but ozone levels are not reduced as much as usual since there are fewer NO_x 's to "eat up" the ozone.

At station T, we find a noticeable grouping of large ozone values when the winds are coming from the east-northeast (fig. 9c). Ozone concentrations of 250 ppb and above are only present when the winds are between 30 and 100 degrees. The occurrence of these large ozone values most likely results because polluted air is carried from the northeast-lying city center and is then trapped by the mountains to the south and west of station T. Ozone concentrations are relatively small when the wind directions are between 180 and 280 degrees, presumably because fresher air is being transported from off the mountains. At station X, we find similar results, although not as well defined (fig. 9d). Ozone concentrations above 200 ppb occur, with one exception, when the wind direction is between 0 and 140 degrees. Although winds from any direction would carry polluted air to station X, winds from the north-northeast would result in trapping of pollutants within the basin and thus perhaps lead to higher levels near the city center. Furthermore, fig. 10 shows that there are no large daytime vector-averaged wind speeds when the wind direction is between 0 and 120 degrees, so that concentrations may be larger, in part, as a result of the lighter winds. The relatively moderate wind speeds may be a result of mountain blocking effects and/or

large-scale synoptic trends associated with northerly flow.

From fig. 9, some simple rules for ozone levels can be devised for each station:

Station F:	if $0 < WD_{11v} < 120$,	then $O_3 > 100$ ppb;
Station L:	if $30 < WD_{11v} < 150$,	then $O_3 > 100$ ppb;
	if $WD_{11v} < 30$ or $WD_{11v} > 180$,	then $O_3 < 150$ ppb;
Station T:	if $WD_{11v} < 30$ or $WD_{11v} > 100$,	then $O_3 < 250$ ppb; and
Station X:	if $WD_{11v} > 140$,	then $O_3 < 200$ ppb.

If contradictions occur when using the two different sets of rules based on $\Delta T/(WS_{11v} + WS_{max})$ and WD_{11v} , we recommend that the rules based on the former quantity be used since grouping of data is better in that case.

Further attempts to improve the grouping of data met with little success. When the daytime-averaged relative humidity and absolute temperature were combined with $\Delta T/(WS_{11v} + WS_{max})$, the scatter in the data increased. Likewise, separating the meteorological data into categories based on the prevailing wind direction led to correlations showing no improvement at best.

Finally, no noticeable improvement in the grouping of data was obtained when ozone was plotted against $\Delta T^n/(WS_{11v} + WS_{max})$, where n was varied between 1/2 and 5/2 in increments of 1/2.

b). Comparison of upper-air meteorological measurements with ozone concentrations

From the upper-air measurements, two important quantities for pollution transport can be derived: the boundary-layer height (H_{bl}) and the near-surface maximum daytime temperature gradient $\Delta\theta/\Delta z$. Unfortunately, their effects on ozone concentration in the Mexico City basin are hard to determine because of the small amount of rawinsonde data that was available to us. Plotting ozone concentration as function of $\Delta T/(H_{bl} (\Delta\theta/\Delta z)(WS_{11v} + WS_{max}))$, we found that correlation improved for stations T and X and became worse for stations F and L. For illustration, the results for stations F and T are plotted in fig. 11. Certainly, with more data points the grouping of data would become more clear.

We also tested ozone's dependence on surface pressure and a bulk near-surface velocity gradient, but found no correlation. When ozone was plotted as function of the vertically-integrated wind speed, instead of the daytime maximum wind speed, no improvement was found in the grouping of data. These results must be interpreted with some caution, however, because of the small number of data points.

5. Summary

The correlation between ozone and meteorological measurements made at four surface stations in the Mexico City basin during the winter months has been studied. We found that ozone

was most strongly correlated to the daytime temperature increase and daytime maximum wind speed. Ozone concentration was an increasing function of the daytime temperature increase, which we proposed was due to ΔT being proportional to the amount of sunlight. Ozone was inversely proportional to the WS_{max} , which most likely results from the turbulent mixing process being proportional to the magnitude of the wind speed. Weaker correlation was found between ozone and the daytime vector-averaged wind speed, an indicator of the net movement of the ozone cloud. Strongest correlation was obtained when ozone was plotted as a function of $\Delta T/(WS_{11v} + WS_{max})$. We also discovered some grouping of data when ozone levels were plotted against the daytime vector-averaged wind direction. From our analysis, we proposed some simple rules for determining upper and lower bounds on the ozone concentrations applicable to all four stations:

if $\Delta T/(WS_{11v} + WS_{max}) < 0.5$,	then $O_3 < 100$ ppb;
if $0.5 < \Delta T/(WS_{11v} + WS_{max}) < 1.0$,	then $O_3 < 230$ ppb; and
if $\Delta T/(WS_{11v} + WS_{max}) > 1.0$,	then $O_3 > 100$ ppb.

and rules applicable at particular stations:

Station F: if $0 < WD_{11v} < 120$,	then $O_3 > 100$ ppb;
Station L: if $30 < WD_{11v} < 150$,	then $O_3 > 100$ ppb;
if $WD_{11v} < 30$ or $WD_{11v} > 180$,	then $O_3 < 150$ ppb;
Station T: if $WD_{11v} < 30$ or $WD_{11v} > 100$,	then $O_3 < 250$ ppb; and
Station X: if $WD_{11v} > 140$,	then $O_3 < 200$ ppb.

Furthermore, we proposed a rule based on only ΔT and WS_{max} for cases where the daytime vector-averaged wind speed was difficult to determine:

if $\Delta T/WS_{max} > 1.5$, then $O_3 > 100$ ppb.

Grouping of ozone concentration data was not improved when the daytime-averaged relative humidity and temperature were combined with the $\Delta T/(WS_{11v} + WS_{max})$ term. Filtering of data by prevailing wind direction did not improve correlations either.

Although it is believed that the boundary-layer height and near-surface potential temperature gradient are important factors in determining ozone concentrations, only a small section was devoted to upper-air measurements because only three weeks of data were available to us. When ozone was plotted as a function of $\Delta T/(H_{bl} (\Delta\theta/\Delta z)(WS_{11v} + WS_{max}))$, we found better grouping of data at stations X and T and more scatter at stations F and L. However, results should be interpreted with caution due to the small size of the data set.

In conclusion, we recommend that more surface data from the winter months be analyzed to validate the simple rules for ozone bounds proposed here. It would be of value to analyze data from different stations and during non-winter months in order to determine if the rules are valid at different locations and times of the year. One of the unmet goals of this study was obtaining a rule for determining when the largest ozone concentrations occur. Analysis of more upper-air data may yield such rules, as large ozone concentrations are often associated with low inversion levels and weak convection at the surface.

Acknowledgments. The author would like to thank Gerald Streit, Mike Williams, and Gary Thayer of Los Alamos National Laboratories for their valuable help in regards to interpreting and processing data. Additionally, I wish to acknowledge the efforts of our colleagues at the Mexican Petroleum Institute and the Secretariat of Social Development for their part in obtaining and distributing the data. Finally, I would like to acknowledge sponsorship from the US Department of Energy Office of Environmental Analysis.

References

Arya, S. P. S. (1988): *Introduction to Micrometeorology*. Academic Press, New York, NY, 320p.

Pasquill, F. and F.B. Smith (1983): *Atmospheric Diffusion*, 3rd ed. Ellis Horwood Limited, Chichester, U.K., 437p.

Seinfeld, J.H. (1986): *Atmospheric Chemistry and Physics of Air Pollution*. John Wiley and Sons, New York, NY, 738p.

Williams, M.D., M.J. Brown, X. Cruz, G. Sosa, and G. Streit (1993): Development and testing of meteorology and air dispersion models for Mexico City. Report no. LA-UR-93-4244, Energy and Environmental Analysis Group, Los Alamos National Laboratory, Los Alamos, NM 87545.

MEXICO CITY TERRAIN

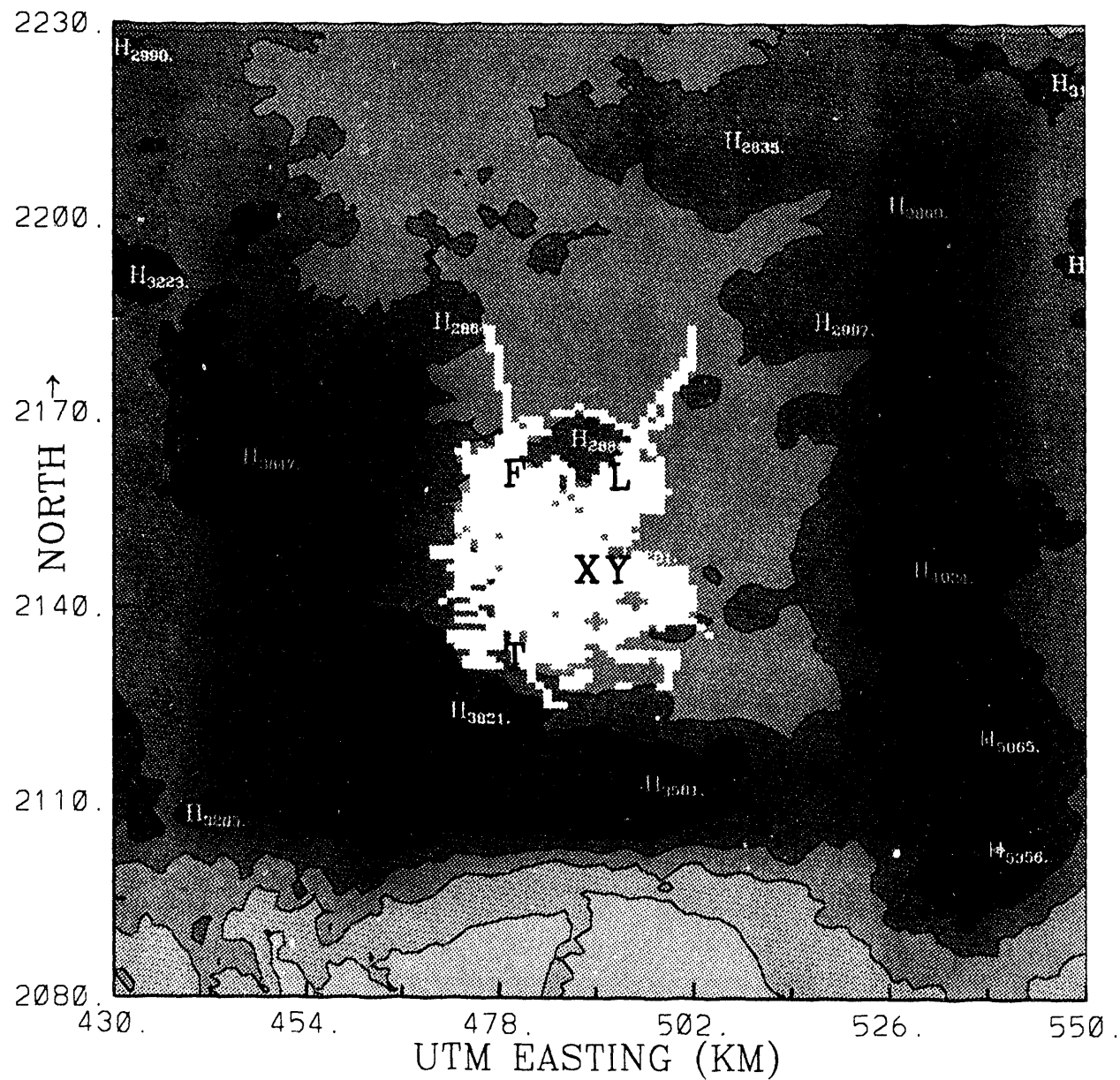


Figure 1. Topographical map of the Mexico City basin. Contour heights range from 1474 to 4925 meters in intervals of 431 meters. The urban area is represented by the yellow region, the surface monitoring stations are denoted by the red letters F, L, T, and X, and the rawinsonde location by the red letter Y.

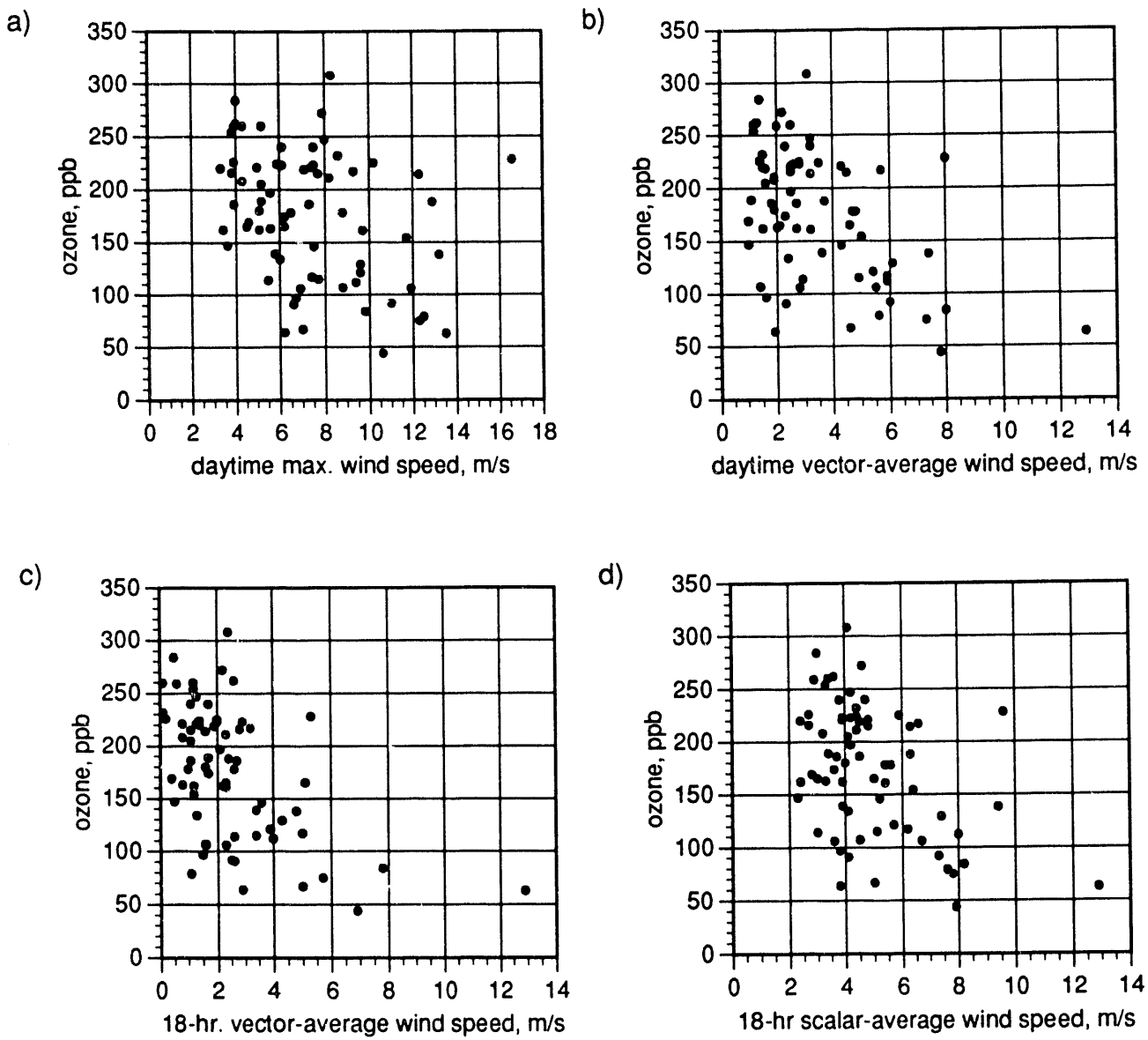


Figure 2. Scatterplots of daily maximum ozone concentration versus wind speed at surface station F for winter months. Comparison of different wind speed variables: a) maximum value measured during the daytime (7:00 am to 6:00 pm); b) vector-averaged during the daytime; c) vector-averaged over eighteen hours (midnight to 6:00 pm); and d) scalar-averaged over eighteen hours.

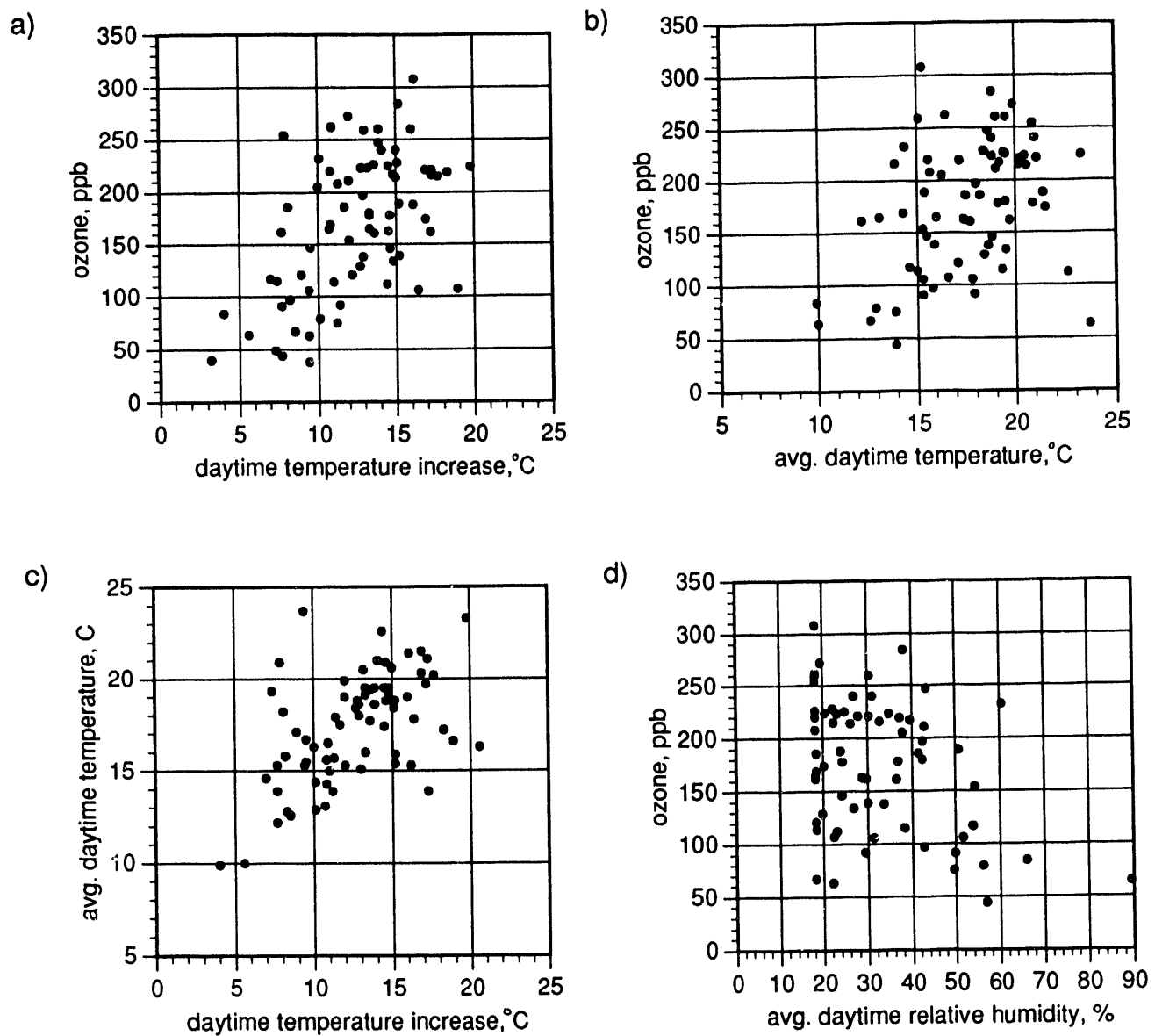


Figure 3. Scatterplots of a) ozone versus daytime temperature increase; b) ozone versus daytime average temperature; c) average daytime temperature versus daytime temperature increase; and d) ozone versus relative humidity at surface station F for winter months.

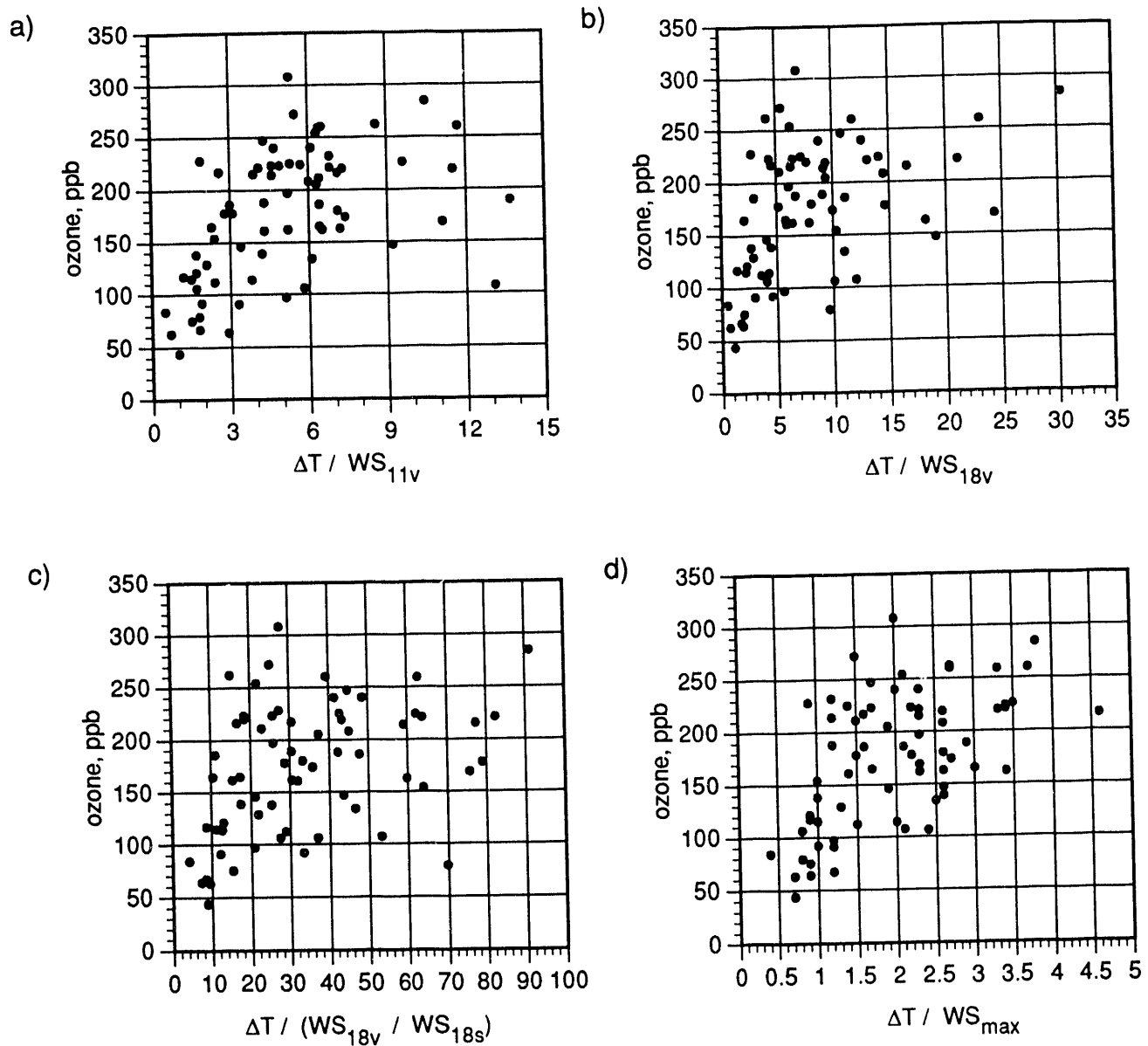


Figure 4. Scatterplots of the daily maximum ozone concentration versus temperature and wind speed variables at surface station F for winter months. Daytime temperature increase divided by: a) daytime (11 hour) and b) 18 hour vector-average wind speed; c) ratio of 18 hour vector-averaged to scalar-averaged wind speed; and d) maximum daytime wind speed.

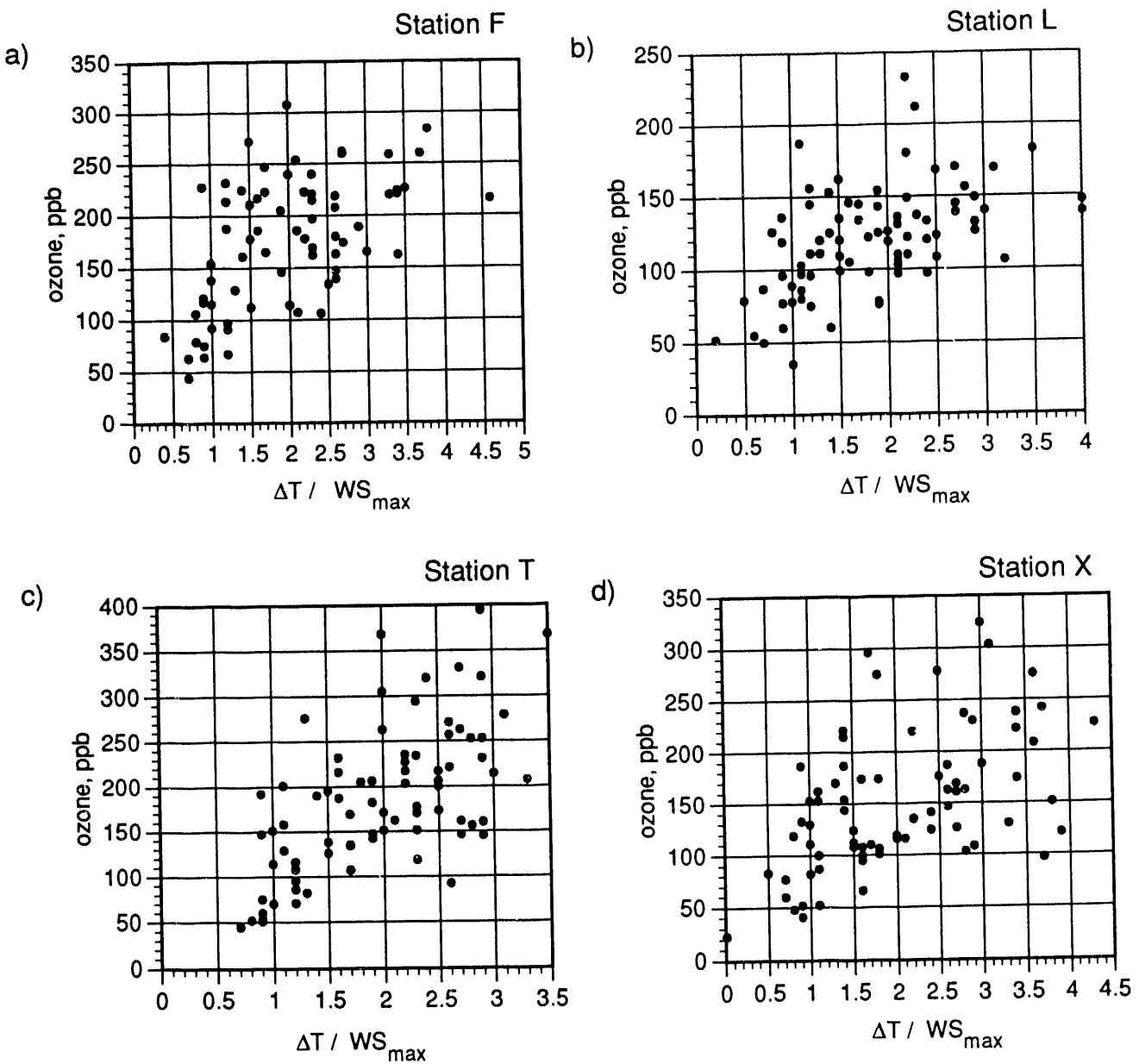


Figure 5. Scatterplots of the daily maximum ozone concentration versus the daytime temperature increase divided by the maximum daytime wind speed. Measurements during winter months at surface stations F, L, T, and X.
 Note: x axis units are $^{\circ}\text{C}/(\text{m/s})$.

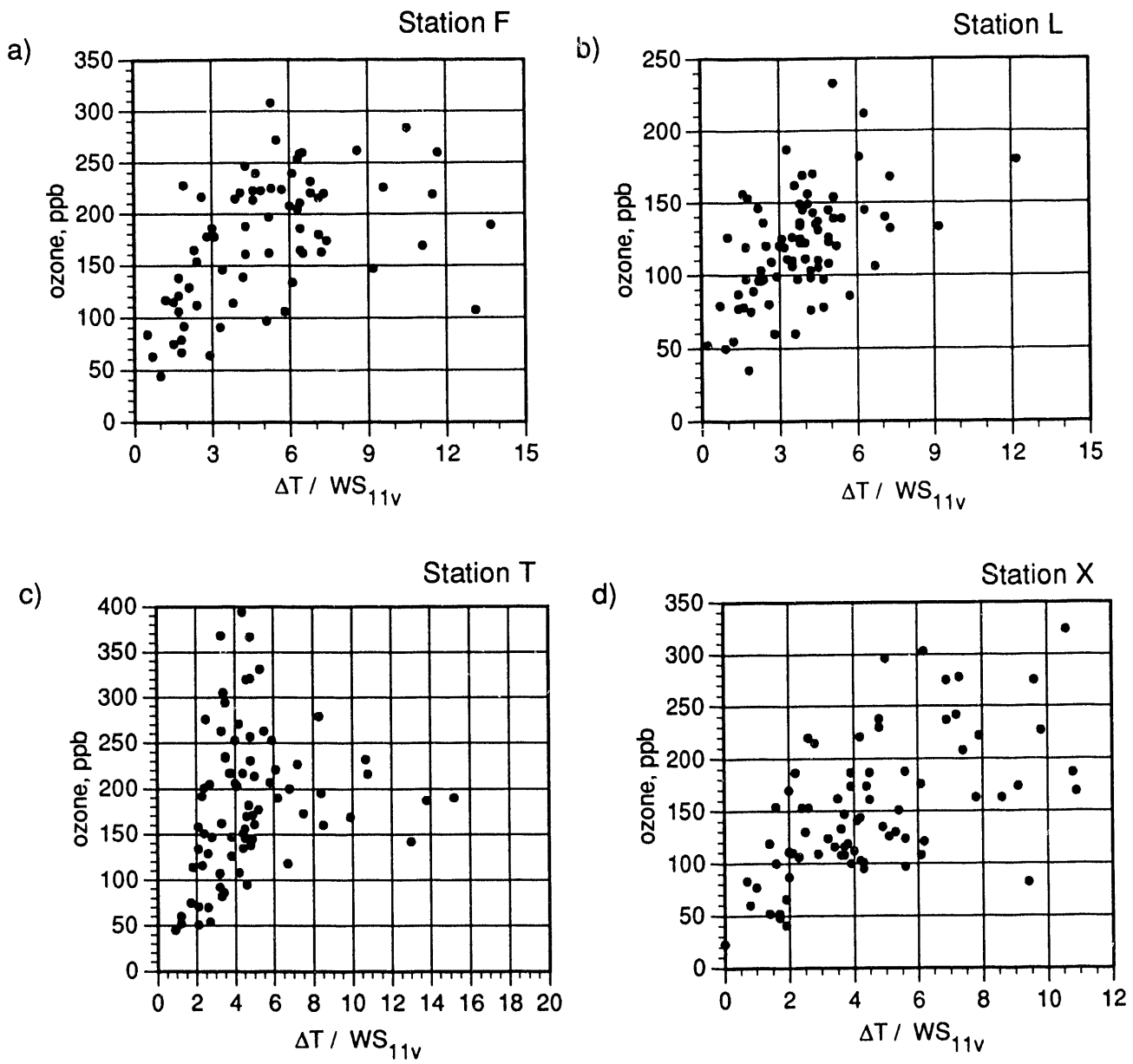


Figure 6. Scatterplots of the daily maximum ozone concentration versus daytime temperature increase divided by the daytime (11 hour) vector-average wind speed. Measurements during winter months at surface stations F, L, T, and X. Note: units of x axis are $^{\circ}\text{C}/(\text{m/s})$.

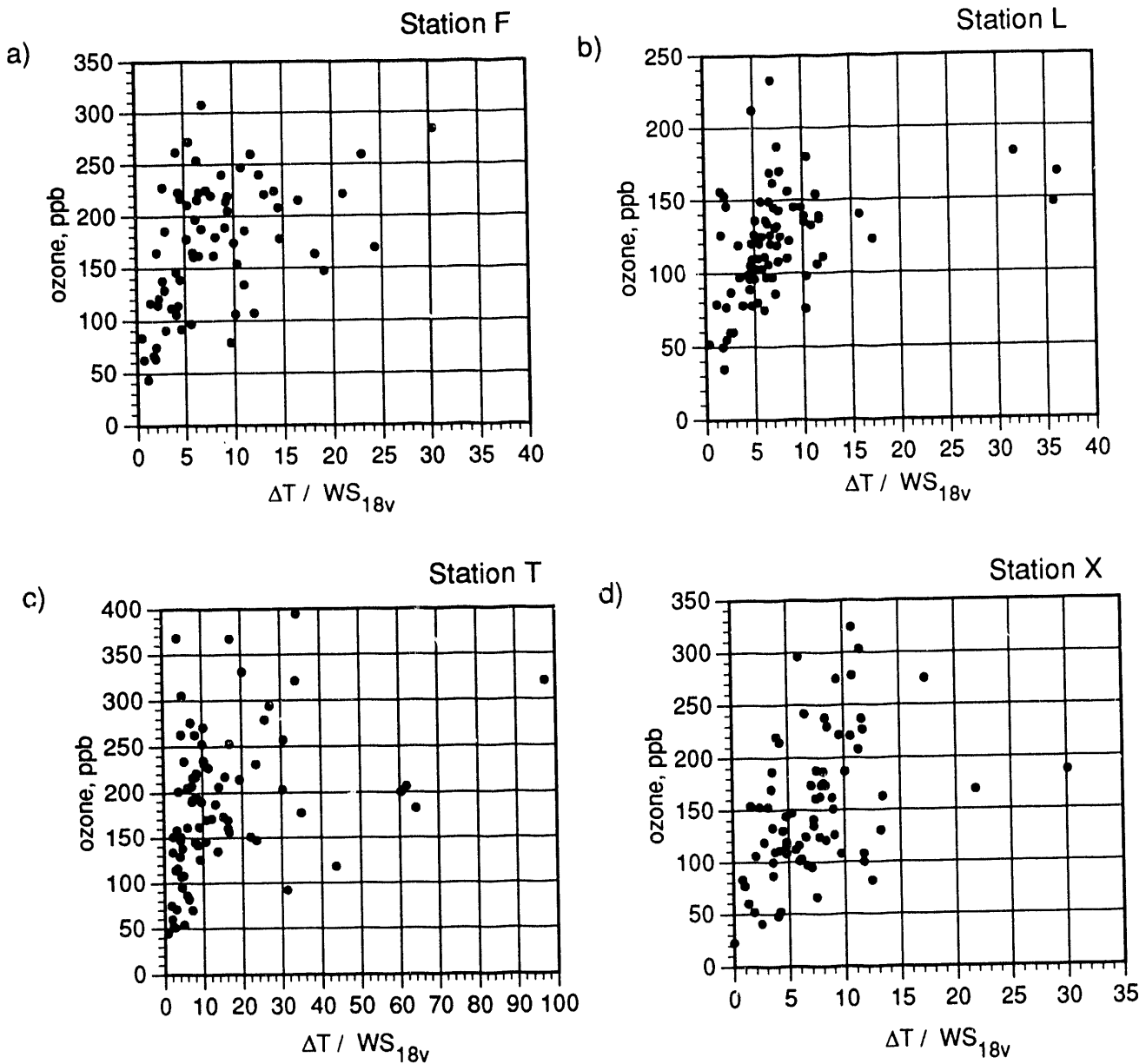


Figure 7. Scatterplots of daily maximum ozone concentration versus the daytime temperature increase divided by the 18 hour vector-average wind speed. Measurements during winter months at surface stations F, L, T, and X. Note: units of x axis are $^{\circ}\text{C}/(\text{m/s})$.

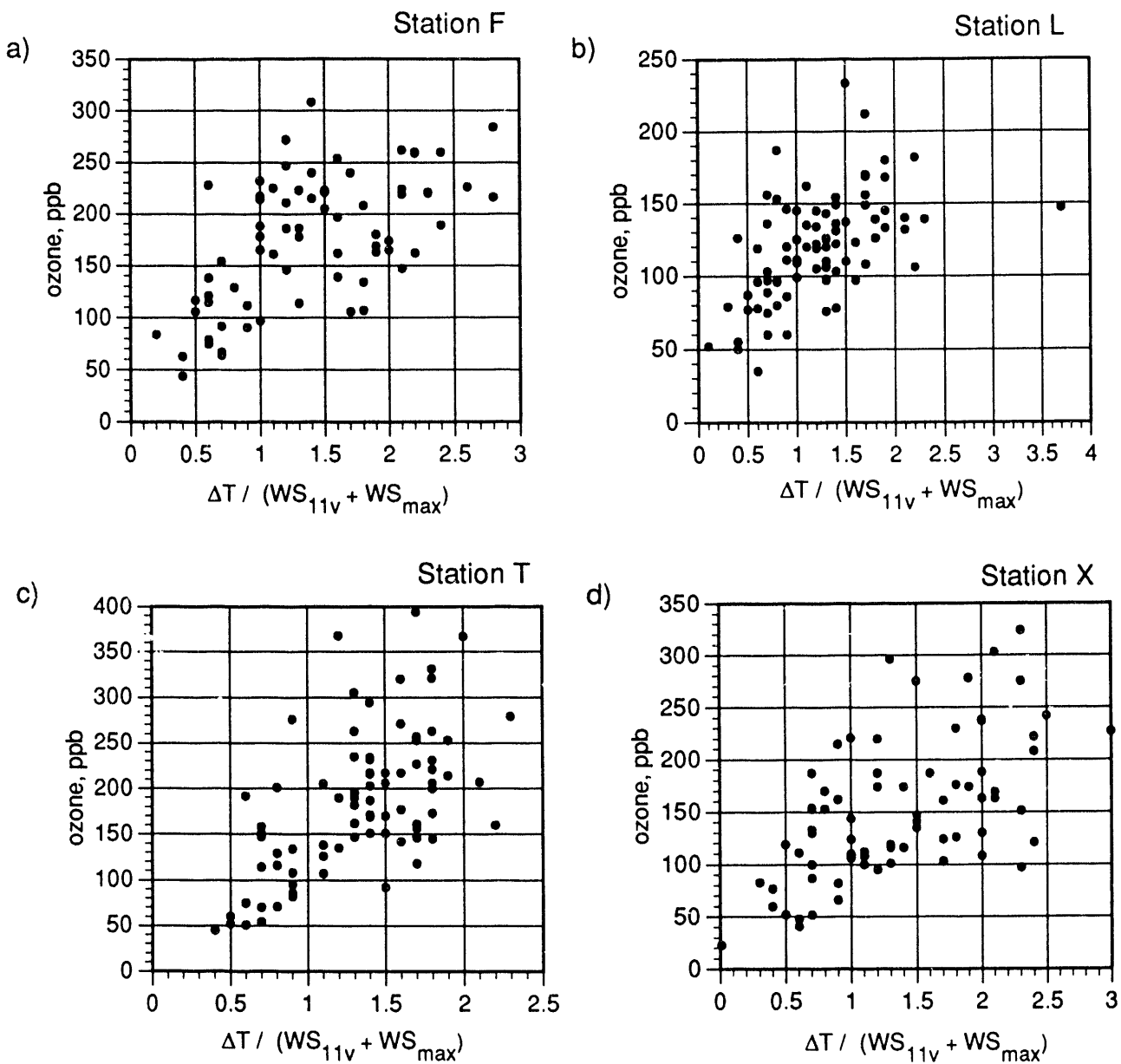


Figure 8. Scatterplots of the daily maximum ozone concentration versus daytime temperature increase divided by the sum of the daytime (11 hour) vector-average and the maximum daytime wind speeds. Measurements during winter months at surface stations F, L, T, and X. Note: units of x axis are $^{\circ}\text{C}/(\text{m/s})$.

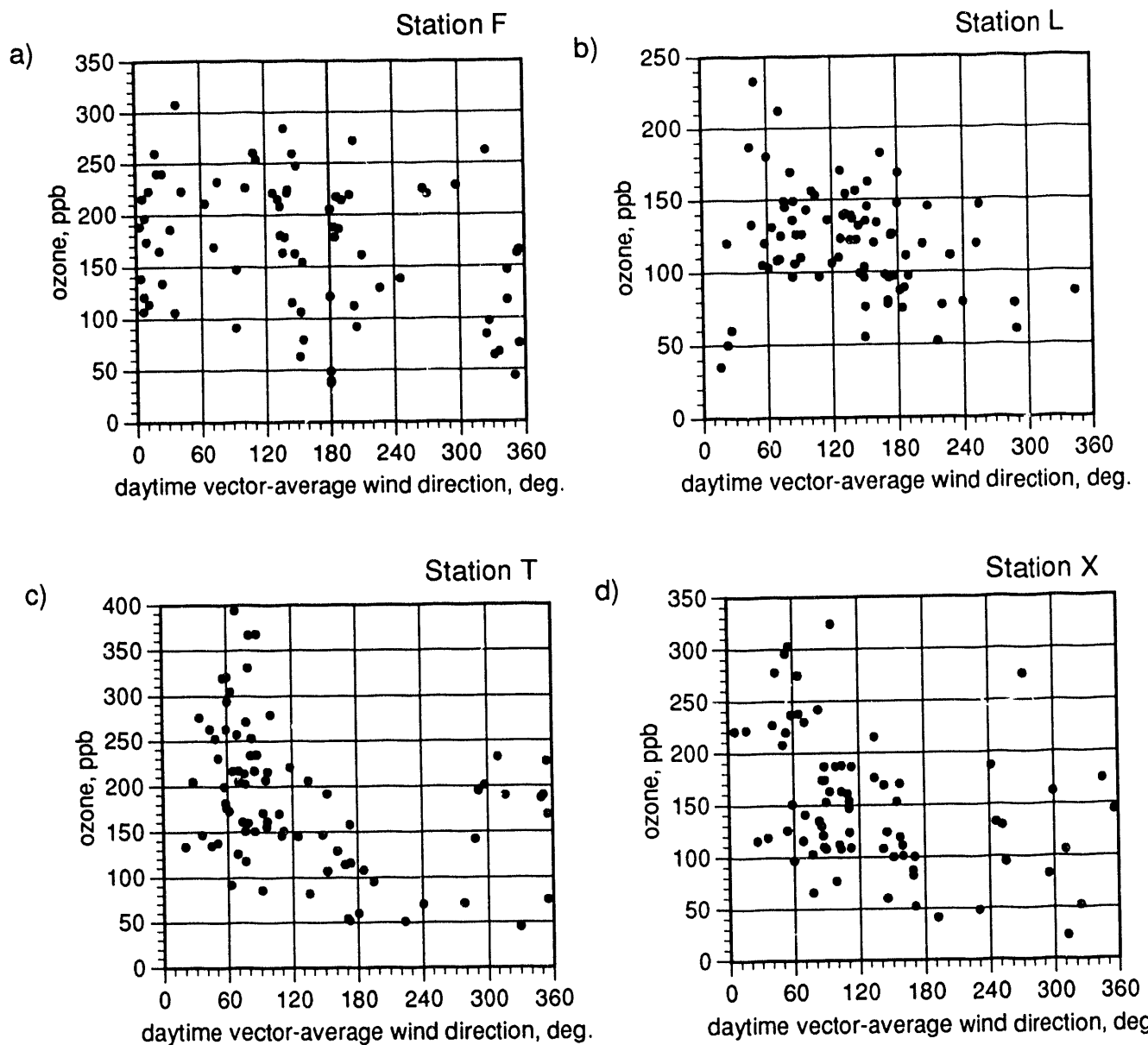


Figure 9. Scatterplots of ozone versus daytime vector-averaged wind direction. Measurements during winter months at surface stations F, L, T, and X.

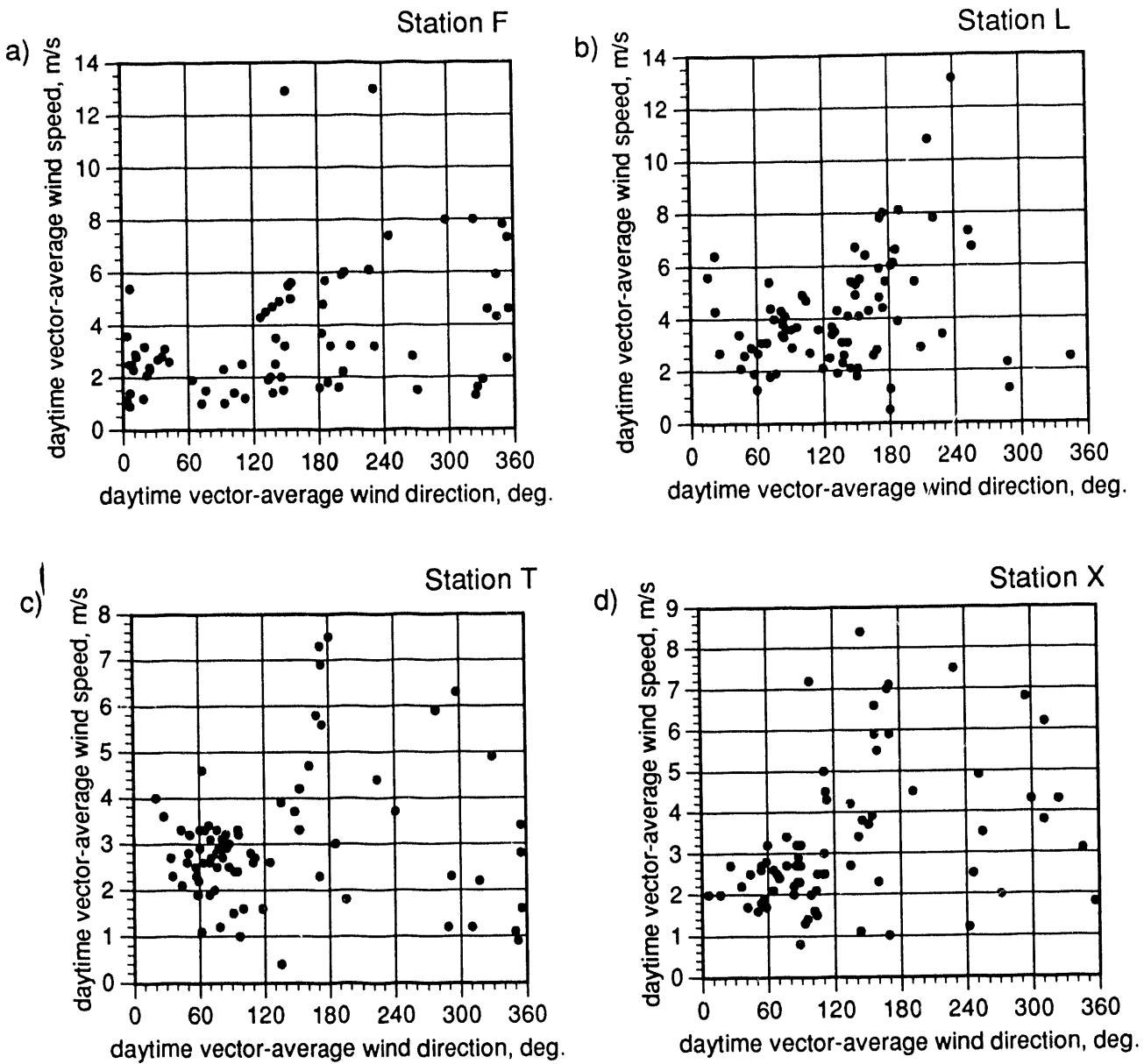


Figure 10. Scatterplots of the daytime vector-averaged wind speed versus wind direction. Measurements during the winter months at surface stations F, L, T, and X.

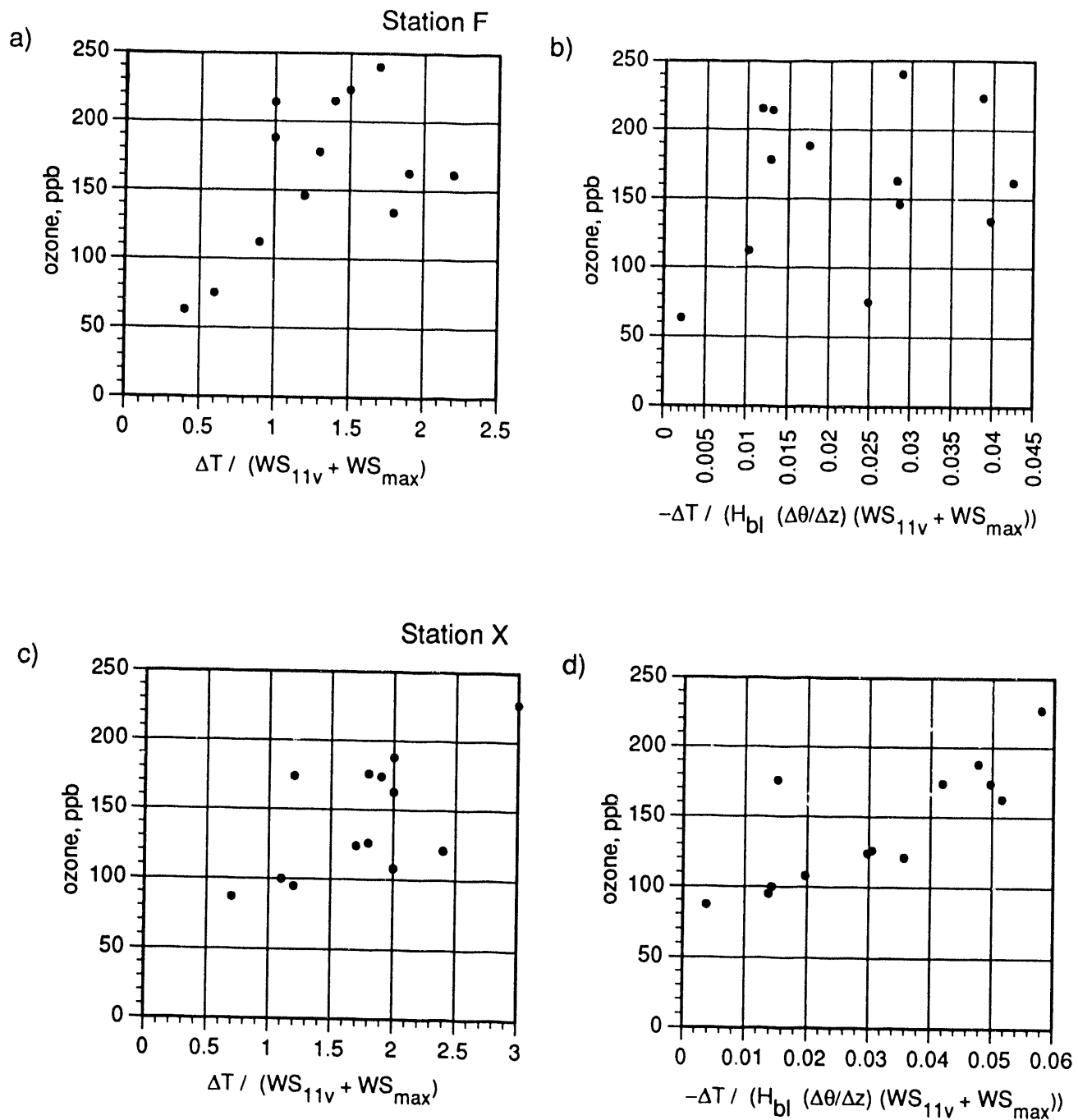


Figure 11. Comparison of scatterplots at surface stations F and X with the daily maximum ozone concentration as a function of: a) & c) daytime temperature increase and daytime vector-average and maximum wind speeds and b) & d) the same, plus boundary-layer height and bulk near-surface temperature gradient. Rawinsonde measurements taken during Feb. 1991. Note: units of x axis are $^{\circ}\text{C}/(\text{m/s})$ in a) & c) and s/m^{**2} in b) & d).

A high-contrast, black and white graphic image consisting of several geometric shapes. At the top, there are four vertical rectangles of varying widths arranged in a staggered pattern. Below them is a long, thin horizontal rectangle. To the right of the horizontal rectangle is a thick, diagonal black bar that slopes upwards from left to right. At the bottom, there is a large, dark, irregular shape that tapers to a point on the left and has a white, irregular shape nested within its lower half.

four / five / six / seven / eight / nine / ten

DATA

